Int J Adv Manuf Technol (2015) 79:2041–2055
DOI 10.1007/s00170-015-6986-5

ORIGINAL ARTICLE

Investigation and optimization of deformation energy and geometric accuracy in the incremental sheet forming process using response surface methodology

Yanle Li · Haibo Lu · William J. T. Daniel · Paul A. Meehan

Received: 20 January 2015 / Accepted: 2 March 2015 / Published online: 14 March 2015

Abstract Incremental sheet forming (ISF) is a promising manufacturing process that features benefits of reduced forming forces, enhanced formability and greater process flexibility. It also has a great potential to achieve economic payoff for rapid prototyping applications and for small quantity production in various applications. However, limited research has been conducted from the sustainability point of view, particularly for energy consumption. More consumed energy will generate more heat and affect tool and product wear. Also, geometric accuracy is still one of the dominant limits for the further development and commercialization of the ISF technology. Therefore, the aim of this study is to investigate how different process parameters affect the consumed energy during the forming process and also find the optimal working condition for lower deformation energy with higher geometric accuracy. A Box-Behnken design of 27 tests for pyramid-forming processes have been performed for a multi-objective optimisation that considers four factors: step down, sheet thickness, tool diameter and wall angle at three levels. The deformation energy during the forming process was calculated based on the measured forming forces. It was found that the deformation energy heavily depends on the sheet thickness because of higher plastic energy required to deform the material. Increasing step-down size within a limited range or decreasing the wall angle is also an effective approach to reduce the deformation energy. Moreover, the effects of various process parameters on the global geometric accuracy have also been investigated. The geometric error has been empirically predicted by quadratic equations giving the influence of the most influential forming parameters. It was concluded that the geometric quality is largely determined by the quadratic effect of wall angle, the linear effect of sheet thickness and the interaction effect of thickness and step down. Finally, the optimal working conditions for both independent and simultaneous minimisation of deformation energy and geometric error during the pyramid-forming process are provided.

Keywords Incremental sheet forming · Box-Behnken design · Response surface methodology · Energy consumption · Geometric accuracy · Optimisation

Y. Li (✉) · H. Lu · W. J. T. Daniel · P. A. Meehan
School of Mechanical & Mining Engineering, The University of Queensland, St Lucia, Brisbane, QLD 4072, Australia
e-mail: yanle.li@uq.edu.au

1 Introduction

In recent years, environmental and sustainability concerns for metal forming processes have brought considerable attention in the academic world. As for the incremental sheet forming (ISF) process, particular interest has focussed on the investigation of the forming efficiency and energy consumption under various process parameters and different machine facilities. ISF technology is an emerging sheet forming process ideal for rapid prototype and small batch production. In the process, a flat metal sheet is gradually formed into the designed 3D shape using computer numerical control (CNC)-controlled generic forming tool. The process is characterized by the fact that at any time, only a small part of the product is formed and the local deformation area moves over the sheet until the desired shape is achieved. By using this process, useable parts can be formed directly from computer-aided design (CAD) data without the use of specialized tooling. Therefore, ISF is widely accepted as a promising forming

process over conventional processes such as deep drawing and stamping for small batch production and custom manufactured products [1, 2].

1.1 Energy consumption

Duflou et al. [3] provided a systematic overview of the energy and resource efficiency improvement methods in the domain of discrete part manufacturing. In terms of the ISF process, three strategies were concluded to reduce the energy usage and improve resource efficiency: (a) redesign of machine tools and selective control, (b) allocating the machine tool at its nominal capacity level and (c) optimising the process parameter settings. Dittrich et al. [4] proposed the concept of exergy analysis (the maximum useful work that can be obtained from a system at a given state in a given environment) in the ISF process and concluded that the exergy of the sheet material contributed a significant fraction to the total exergy input. Also, compared with conventional forming and hydroforming processes, ISF is advantageous for prototyping and small production runs up to 300 parts from an environmental point of view. Branker et al. [5] firstly analysed the cost, energy and carbon dioxide emissions in a single point incremental forming (SPIF) process for manufacturing a custom-designed aluminium hat. By doubling the feed rate and step-down size, as well as using an eco-benign lubricant, it was found that the cost and energy used during the process without labour reduced from $4.48 to $4.10 and 4580 to 1420 kJ, respectively.

Ingarao et al. [6] analysed the energy consumption during both the traditional stamping and the ISF process based on the measured forming forces. The focus was to investigate both the efficient use of materials and process energy saving. It should be noted that the energy consumption was calculated from the recorded forces in all three orthogonal directions multiplied by the corresponding travel distance of the forming tool in that direction. One conclusion has been drawn that the required deformation energy in the ISF process is always higher than that for stamping for all the considered cases, although the ISF process allows a certain material saving. Also, it is suggested that the energy reduction could be obtained through varying the material type, part shape as well as thickness. The empirical evidence presented in this paper provides useful comparison guidelines for materials saving and energy consumption but the optimal solution is not discussed. Recently, Ingarao et al. [7] comprehensively analysed and compared the electric energy consumption of the ISF process by using three different machines: a CNC milling machine, a six-axis robot as well as the dedicated AMINO machine tool. Working cycle time and power studies were conducted for all three setups. In terms of the effect of material type of the workpiece, no difference in power demand was observed for CNC milling machine but the six-axis robot was proved to be sensitive to the material type. The AMINO setup is the most efficient machine tool in terms of instantaneous power but requires higher total electric energy due to the lower forming speed compared with the six-axis robot. As far as the process parameters are regarded, the strategy to reduce the forming time by increasing feed rate and step-size within the admissible range was recommended as the most effective approach to reduce the energy consumption. In addition, the authors also presented a parametric model to predict the energy consumption for the robot-based ISF operations by simply considering the ultimate tensile strength of the material and the processing time. It should be noted that this model highly depends on the predicting accuracy of the steady vertical force from previous work [8].

Ambrogio et al. [9] compared the power consumption of the SPIF process with two setups: a CNC milling machine and a CNC turning machine. A constant power trend was recorded during the forming step for all the tests due to the fact that loads required to deform the material are much lower than the ones required for the normal operation of machining. It is suggested that the forming time is the dominant factor for energy consumption in the SPIF process. Using the same setup, by reducing the forming time from 144 to 12 s, the energy consumption can be effectively reduced from 838 to 103 kJ. Also, a proper selection and use of machine setup could lead to further saving of energy consumption. Bagudanch et al. [10] studied the effect of process parameters on the energy consumption in the ISF process. A series of experiments were conducted by considering sheet material, step down as well as the tool rotation speed while keeping feed rate as constant. Interestingly, it was concluded that the variation of tool rotation speed is the most significant parameter, followed by the material of the workpiece and incremental step size. It is explained that the lower rotation speed greatly reduced the friction between the sheet and the tool and also decreased the processing time since the rotation has to be stopped when the tool descends to the next contour for the machine setup. Unfortunately, the investigated process parameters were only varied at two levels which should be further extended to provide more comprehensive conclusions.

1.2 Geometric accuracy

Presently, the geometric accuracy for ISF products is still one of the biggest challenges for both academic researchers and industrial users. Allwood et al. [11] reported that the specification of geometric accuracy from industrial users for metal sheet components are typically within ±0.2 mm over the whole surface of a part, while the geometric error for ISF currently only achieved around ±3 mm. They [12] also summarized the geometric accuracy in the ISF process into three definitions, i.e. (a) clamped accuracy, (b) unclamped accuracy

and (c) final accuracy. Research is mainly aimed at improving the clamped accuracy. Micari et al. [13] further categorized the shape accuracy of ISF into three different typologies as shown in Fig. 1: (a) sheet bending close to the major base of the part where plastic deformation starts, (b) sheet springback after the forming tool is lifted after forming and (c) pillow effect on the minor base of the product.

The effects of process parameters on geometric accuracy have been investigated through both numerical modelling and experimental methodology. Essa and Hartley [14] found that the sheet bending near the initial tool contact location can be minimised by the backing plate; the springback can be reduced by the kinematic tool; and the pillow effect can be eliminated by extending the tool path across the base of the sheet. Guzmán et al. [15] simulated a two-slope SPIF pyramid with two different depths using the FEM to investigate the geometric deviation at the slope transition zone. It is concluded that elastic strains due to structural elastic bending were the main causes of the shape deviations. The localized springback has only minor contribution because no plastic deformation is observed in the angle transition zone.

Ambrogio et al. [16] statistically analysed the effects of process parameters of tool diameter, depth step, wall angle, final product depth and the sheet thickness on geometric accuracy of the formed truncated cone. It was suggested that the geometric error measured at the corner was largely influenced by sheet thickness and total part depth. On the other hand, the pillow effect at the middle of the base was strongly affected by the tool diameter and product height. Ham [17] performed a Box-Behnken design with 46 experimental tests considering 5 factors (material type, sheet thickness, tool size, step size and formed shape) varied at 3 levels to study their effects on dimensional accuracy. It is observed that the geometric deviation at the bottom of the formed shape is small compared with the remaining area, and the overall geometric error for most of the parts is within 1 mm after a user-defined scale. However, only qualitative comparisons were provided based on several contour plots of geometric deviations in this study, and further qualitative investigation is required.

The above literature suggests that the total energy consumption in an ISF process includes machine standby energy, positioning energy and deformation energy. The machine standby energy and positioning energy highly depend on the type of machine used for the process and have no direct relation with the process parameters. The deformation energy is directly related to the heat generation and also wear to the tool and the formed material. Therefore, deformation energy is focused on for investigation in the present work. Although substantial research work has been conducted on the clamped accuracy, the degradation in unclamped and final accuracy due to residual stresses in the sheet has had very little attention in the literature. Therefore, the effects of process parameters on the unclamped accuracy should be further investigated. Additionally, there is still a lack of comprehensive research on the simultaneous optimization of energy consumption together with other process quality outputs such as geometric accuracy taking into account the effects of the most relevant process parameters. Based on the extensive review of the current status of ISF, the aims of the present work are set as follows:

- To perform a series of systematic tests using response surface methodology (RSM) with Box-Behnken design to study the effects of the most relevant process parameters (step down, sheet thickness, tool diameter and wall angle) on both deformation energy and geometric accuracy by forming the shape of truncated pyramid.
- To develop empirical models for predicting consumed energy and geometric error individually using response surface methodology based on the experimental results obtained. The effect of each factor on these two responses will be analysed in detail.
- To optimise the deformation energy and geometric error independently and simultaneously using the desirability function. The optimal working conditions for these optimisations will be provided.

2 Methodology

The details of experimental facilities, determination of deformation energy and geometric error and the experimental design procedure adopted for the study are described in this section.

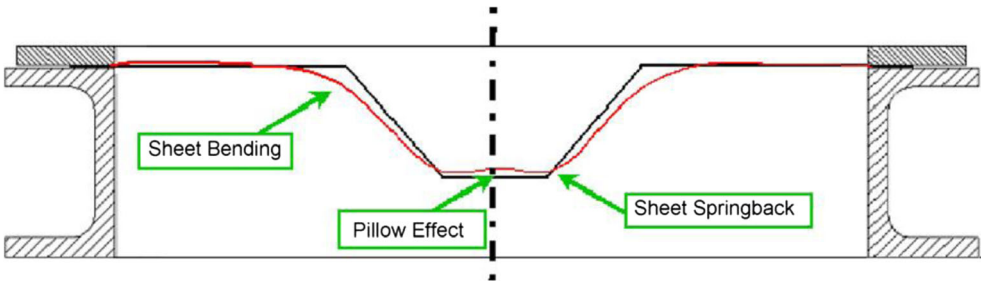

Fig. 1 Geometrical errors during the SPIF process [13]

2.1 Experimental setup

The forming tests were performed on a state-of-the-art AMINO machine dedicated for the ISF process as shown in Fig. 2. The machine allows mould-based forming for a maximum size of 2100 mm×1450 mm×550 mm with a FANUC controller for precise control. The movement of the two horizontal axes (*X* and *Y*) can have a maximum speed of 60 m/min with a repeatability of ±0.05 mm. The vertical (*Z*) axis is driven by an AC servo motor with the power of 1 kW that allows a maximum acting force of 3 kN. Hemispherical tools with the diameters of 10, 20 and 30 mm were used to deform the material. The tip of each tool is tungsten carbide and the body is made of K110 steel which was hardened and tempered to HRC60. The forming tool was set not to rotate in this study for all the tests. The material used in the present study was aluminium alloy 7075-O sheets with three different thicknesses which were cut into 300 mm×300 mm-sized samples.

The geometry of a truncated pyramid was selected as the targeted shape to facilitate the calculation of consumed energy and evaluation of geometric accuracy. The four investigated process parameters are step down, sheet thickness, tool diameter and wall angle. The definition of these parameters and the configuration of the forming process are illustrated in Fig. 3. The vertical distance between each neighbouring contour is defined as step down, and the angle between the deformed sheets to the horizontal plane is defined as wall angle. Before forming, the sheet was clamped on the frame with 12 evenly distributed blank holders. During the forming process, the forming tool was numerically controlled by a FANUC controller which follows the previously designed tool path. The contact between forming tool and metal sheet was lubricated by Shell Tellus Oil 68 to reduce friction and avoid excessive wear of the tool surface.

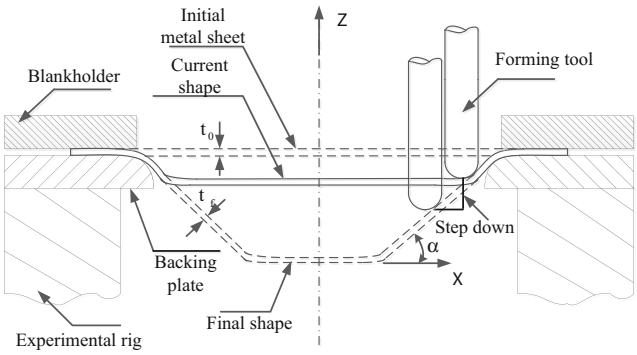

Fig. 3 Sketch of ISF experimental configuration and associated parameters [18]

2.2 Calculation of deformation energy

The deformation energy was calculated based on the measured force components [6]. It should be noted that the deformation energy investigated in the present study is only the theoretical one that is different from the actual electric energy consumed by the machine. Although the deformation energy is only part of the total electric energy, it is directly related to the change of process parameters. Therefore, the study of deformation energy is critically helpful for the understanding of the actual deformation behaviour of the material under different process conditions during the forming process. The total deformation energy is constituted by three components E_x, E_y and E_z corresponding to three orthogonal forming forces *Fx*, *Fy* and *Fz*, respectively. As shown in Fig. 2b, a multiple-axis force sensor K6D175-50 was used to measure the forces between the tool and workpiece during the forming process. The force sensor was manufactured by ME-Meßsysteme GmbH which allows measurement of the three orthogonal forces and three torque components at the same time. To alleviate the possible deflection from other structures, the force sensor

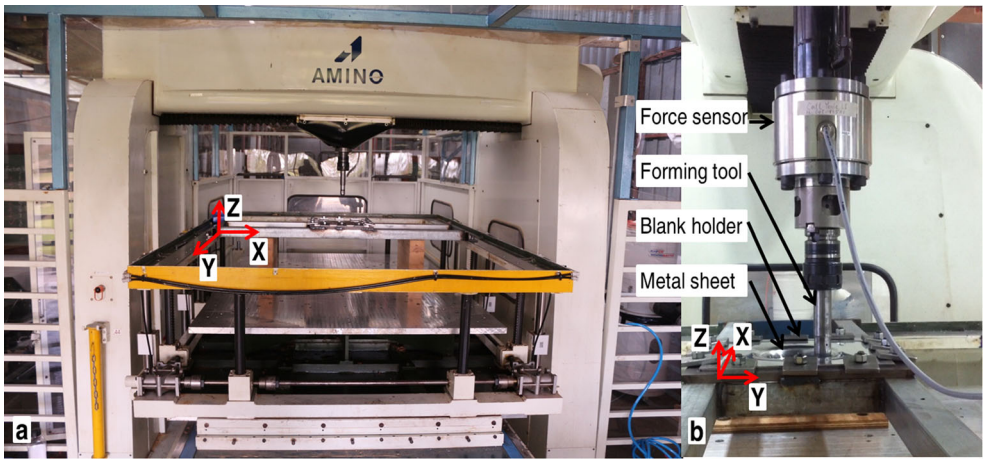

Fig. 2 The AMINO incremental forming machine and the implemented force sensor: **a** front view; **b** detailed side view

was mounted directly between the spindle and the tool holder. The six-channel output signals were recorded with two NI 9237 data loggers and post-processed with the LabVIEW SignalExpress software.

Figure 4 presents typical measured force components for a pyramid-forming process. It is noted that, during the *i*th contour, forming forces during forming of the four straight sides are steady and with only sudden peaks at corners (as marked in Fig. 4). Therefore, the work done by two horizontal force components can be estimated by the average force at each contour multiplied by the travel distance at the corresponding direction of the forming tool. For the vertical component, the energy is only produced when the tool increments to the next contour. As a result, the deformation energy at the *i*th contour can be calculated as follows:

$$E_i = 2F_{xi} \cdot f \cdot t_{xi} + 2F_{yi} \cdot f \cdot t_{yi} + F_{zi}\Delta z, \quad (1)$$

where f is the feed rate of the forming tool, t_{xi} and t_{yi} are the forming time in x and y directions at the ith contour and Δz is the step-down size. Then the total energy to the nth contour can be obtained as follows:

$$E_{total} = \sum_{i=0}^{n} E_i, \quad (2)$$

where n is determined by the formed depth H and step-down size as $H/\Delta z$.

2.3 Measurement of geometric error

To evaluate the geometric accuracy, the 3D geometry of formed parts in an unclamped condition was measured using a noncontact 3D digitiser (VIVID 9i), as shown in Fig. 5. The scanning accuracy is within ±50 μm, which was used in the literature for geometric accuracy previously [19]. GEOMAGIC Qualify was used to process the 3D geometry data from the scanned shape and analyse the dimensional error between deformed test parts and designed CAD models. Specifically, both produced and designed profiles were represented in large sets of points in the same Cartesian coordinate system. In this work, the shape of truncated pyramid is selected as the target shape, and the four investigated process parameters of step down, sheet thickness, tool diameter and wall angle are presented in Fig. 3. The cross-sectional profile through the pyramid centre and perpendicular to the edges was used to evaluate the geometric accuracy. The deviation in vertical direction (Z) between the designed and fabricated profiles as shown in Fig. 9 was calculated as the global geometric error for subsequent investigation. Before scanning, the surface of the parts needs to be sprayed with white powder to avoid light refection as shown in the marked sample in Fig. 6.

2.4 Response surface methodology with Box-Behnken design

Response surface methodology (RSM) was employed in the present work to model and optimise the effects of four independent variables on deformation energy and geometric error during the ISF forming process. RSM is an empirical modelling technique that can help to investigate the interactive effects of process variables and to build a

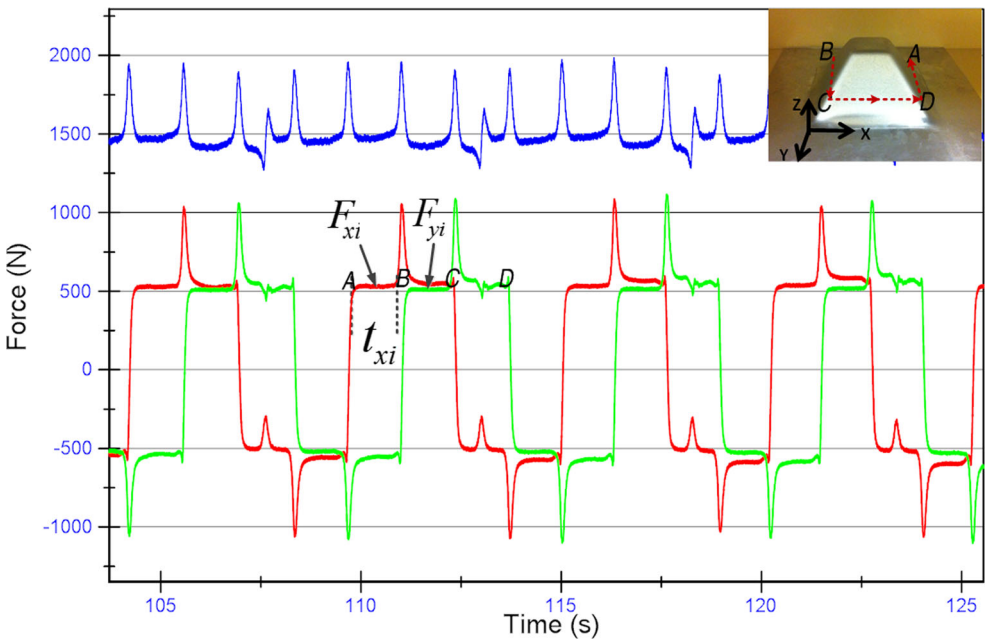

Fig. 4 Typical force components during the pyramid-forming process

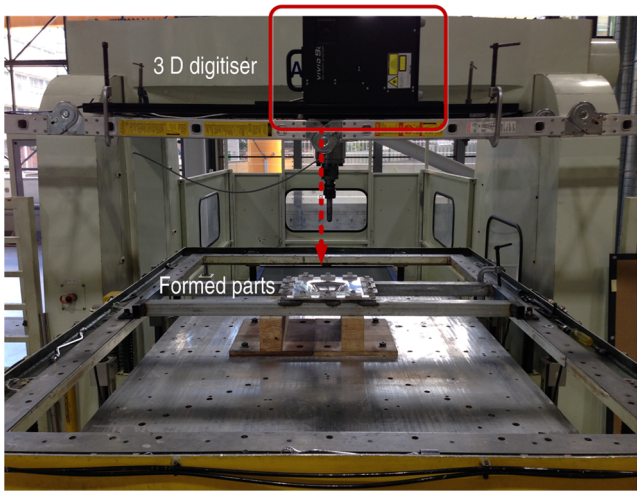

Fig. 5 Set-up of the 3D digitiser

mathematical model that accurately describes the overall process [20]. This optimisation process involves three major steps: (i) performing statistically designed experiments, (ii) estimating the coefficients in a mathematical model and (iii) predicting the response and checking the adequacy of the model [21]. The most common and efficient design used in response surface modelling is the Box-Behnken design. This design allows efficient estimation of the first- and second-order coefficients between the response and selected factors. Since Box-Behnken designs have fewer design points, they are less expensive to run than other designs with the same number of factors. This design was also proved to be feasible for ISF process by many researchers [17, 22, 23]. Hence, a Box-Behnken experimental design was conducted to evaluate the effects of process parameters on deformation energy and geometric accuracy. The steps in this research work for the experimental investigation include the following [24]:

Fig. 6 Truncated pyramids by incremental sheet forming

- Identifying the important process control variables. In this case, based on previous experimental work, four process parameters of step down, sheet thickness, tool diameter and wall angle were selected as the most relevant factors. Previous research has found that increasing the feed rate (forming speed) can effectively reduce the total energy [9] and has no considerable effect on the part quality regarding the formability and surface roughness [25]. To emphasize the effects of other factors, the feed rate has been set as constant at 4000 mm/min in the present study. Although sheet thickness and wall angle may not be changeable according to the manufacturing requirement, they directly influence the contact condition during the process so the investigation of these factors will benefit the understanding of the deformation mechanics in ISF.
- Finding the upper and lower limits of the control variables. Three levels of each factor were considered and their upper and lower values were set as listed in Table 1.
- Development of the design matrix using Box-Behnken design and conducting the corresponding experiments. A total of 27 experimental tests were designed using Minitab Version 16.2.4 in the presented study.

3 Results and discussion

This section first provides the experimental results of deformation energy and geometric error for each test according to the Box-Behnken design. Then, the effect of each factor on both energy and geometric error are discussed in detail followed by the optimisation of these two design responses during the pyramid-forming processes.

3.1 Design of experiments

The Box-Behnken design was applied using Minitab software based on the selected factors and values in Table 1. A design matrix with 27 experimental runs was generated as listed in Table 2. Experiments were conducted in sequence to mitigate the influence of non-considered factors. Due to the fact that parts with

Table 1 Process parameters and their levels

Symbols	Factors	Levels			Units
		−1	0	1	
A	Step down	0.5	1.0	2.0	mm
B	Sheet thickness	1.27	1.80	2.54	mm
C	Tool diameter	10	20	30	mm
D	Wall angle	50	60	70	degree

70° wall angle were not successfully formed to the designed depth of 65 mm, the deformation energy for forming until a depth of 24 mm was calculated and analysed for all the cases. In terms of the geometric accuracy, the successfully formed parts were compared with the designed shape, while the fractured parts were compared with the supposed intermediate shapes corresponding to the final formed tool path. Deformation energy and geometric error are the design responses and their calculated values for each test are presented in Table 2. Figure 6 shows the formed pyramid parts according to the Box-Behnken design matrix, with the last sample sprayed with white powder for geometric scanning.

3.2 Deformation energy

An empirical relationship between deformation energy and the four studied factors was obtained from the Box-Behnken design results. In the following analysis, factors are considered as their coded values as given in Table 1. This is because coding eliminates any spurious statistical results due to different measurement scales from factors (e.g. step down versus degrees). Additionally, using uncoded units often leads to colinearity among the terms in the model. This inflates the variability in the coefficient estimates and makes them difficult to interpret. Consequently, the statistical equation for the relation between deformation energy and selected coded parameters was derived as follows:

$$E = 4205.32 - 1652.69A + 2018.26B - 568.51C + 701.54D + 1030.47A^2 + 624.27C^2 - 637.57AB - 269.23AC - 207.26AD + 338.38BD, \quad (3)$$

Table 2 Box-Behnken design for four factors and observed responses

Test run no.	Step down (mm)	Sheet thickness (mm)	Tool diameter (mm)	Wall angle (°)	Formed depth (designed) (mm)	Deformation energy (J)	Global geometric error (mm)
1	0.5	1.27	20	60	65	4273.85	2.749
2	2	1.27	20	60	65	2169.40	2.635
3	0.5	2.54	20	60	65	9801.50	4.137
4	2	2.54	20	60	65	5065.90	4.947
5	1	1.8	10	50	65	5099.50	2.204
6	1	1.8	30	50	65	3991.70	3.049
7	1	1.8	10	70	27	6286.40	1.620
8	1	1.8	30	70	31	5346.70	1.938
9	0.5	1.8	20	50	65	5574.40	2.818
10	2	1.8	20	50	65	2887.50	3.239
11	0.5	1.8	20	70	26	7414.20	1.218
12	2	1.8	20	70	30	3831.20	2.233
13	1	1.27	10	60	65	3550.60	2.639
14	1	2.54	10	60	33	8500.00	2.743
15	1	1.27	30	60	65	2904.50	2.676
16	1	2.54	30	60	65	7271.50	4.672
17	0.5	1.8	10	60	65	7225.80	2.860
18	2	1.8	10	60	65	4856.00	3.584
19	0.5	1.8	30	60	65	6799.60	3.187
20	2	1.8	30	60	65	3290.50	3.756
21	1	1.27	20	50	65	2503.10	2.491
22	1	2.54	20	50	65	5925.30	3.787
23	1	1.27	20	70	24	3435.00	2.391
24	1	2.54	20	70	33	8191.60	2.825
25	1	1.8	20	60	65	4492.20	3.699
26	1	1.8	20	60	65	4450.50	3.516
27	1	1.8	20	60	65	4569.70	3.7977

where variables A to D are defined in Table 1. The significance of the developed response function is examined from the following aspects. First, the analysis of variance (ANOVA) is adopted to evaluate the fitness of the established model and also the importance of factors to the response. Table 3 presents the results of ANOVA of the response function surface. The present analysis is carried out at a level of confidence of 95 %. Accordingly, if the *P* value is less than or equal to 0.05, then the effect of the corresponding factor on the response is considered significant. As shown in Table 3, with a probability *P* value less than 0.0001 for the established model, it is indicated that the developed second-order response function is sufficiently adequate. Second, the residuals versus their expected percentiles are plotted in Fig. 7 to examine if the distribution is normal. In this figure, the abscissa represents the residuals between the measured and predicted values and the ordinate stands for the percentage of the measurements that fall below the residuals. If the data is distributed normally, the plot of the residuals should be linear. Since the experimental results are approximately a straight line in Fig. 7, it is confirmed that the model is effective. Moreover, the value of predicted R^2 is used to measure the prediction ability of the developed model. In this analysis, a value of 0.996 of predicted R^2 suggests that the model can be reasonably used for future prediction.

According to the *P* values in Table 3 and coefficients in Eq. (3), all four parameters, especially the sheet thickness, are found to have significant linear effect on the energy consumed for forming the pyramids. Additionally, the quadratic effects of the step down (A^2) and tool diameter (C^2) are also compelling as well as two-level interaction effect of step down and thickness (*AB*). The response surface plots of deformation energy with different factors are presented in Fig. 8 to facilitate the investigation of their individual influences. In each sub-figure, the response is constructed by two experimental factors while holding the remaining two at the middle level. Since further examinations show that the response trends for holding at different levels are similar, it is reasonable to analyse the effect of each factor by the figures given below.

Table 3 Results of ANOVA for global deformation energy (from Minitab)

Source	SS	DOF	MS	*F* value	*P* value	Remarks
Model		14		265.91	<0.0001	Significant
A		1		1172.02	<0.0001	Significant
B		1		1590.61	<0.0001	Significant
C		1		121.84	<0.0001	Significant
D		1		185.53	<0.0001	Significant
A^2		1		157.56	<0.0001	Significant
B^2		1		1.3	0.277	
C^2		1		76.79	<0.0001	Significant
D^2		1		0.39	0.542	
AB		1		65.69	<0.0001	Significant
AC		1		11.5	0.005	Significant
AD		1		6.82	0.023	Significant
BC		1		3.12	0.103	
BD		1		17.23	0.001	Significant
CD		1		0.26	0.619	
Residual		12				
Lack of fit		10		8.68	0.108	
Total		26				

In Fig. 8, it can be seen that the deformation energy under different working conditions are varied over a large range from 2000 J to more than 9000 J, so the investigation of how different process factors affect the required energy is critical for the sustainable development of the ISF technology. The effect of sheet thickness (*B*) is analysed as the most significant factor associated with deformation energy during the pyramid-forming process. Figure 8a, d, e show the response surface of deformation energy with the variation of sheet thickness with step down, tool diameter and wall angle, respectively. All these figures have clearly confirmed that the required deformation energy increases with the increase of the sheet thickness. This is because thicker sheets require larger forming forces to achieve the same amount of plastic deformation. More specifically, the increase of deformation energy appears to be linearly proportional to the rise of the sheet thickness. This was confirmed by both experimental measurements and theoretical analysis. Previous experimental results [26] showed that the tangential forming force is linearly proportional to the sheet thickness in the forming of the truncated cone. Moreover, according to the calculation of plastic deformation power in [27], the power has a linear relation with the sheet thickness under both shear and stretching deformation modes. Therefore, when the shear and stretching deformation modes are dominant, it is reasonable to observe a linear response of deformation energy with varying sheet thickness.

The effect of wall angle on the deformation energy can be approximately treated as a linear effect based on the observation from Fig. 8c, e, f. Parts with larger wall angles require more energy to produce. However, due to the interaction effects of *AD* and *BD*, the slope of the response surface with the change of wall angle in these three conditions are varied, but the most evident cases occur with lower values of step down in Fig. 8c and thicker sheet thickness in Fig. 8e.

It is clearly illustrated from Fig. 8a to c that the increase of the step-down size (*A*) will result in a substantial reduction of deformation energy, which is evidenced in both Eq. (3) and *F* value in Table 3. Although the quadratic term of step down has a positive influence on the required energy, it is counteracted by a more significant negative effect from the linear term. This is explained by the fact that reduction of the number of forming contours

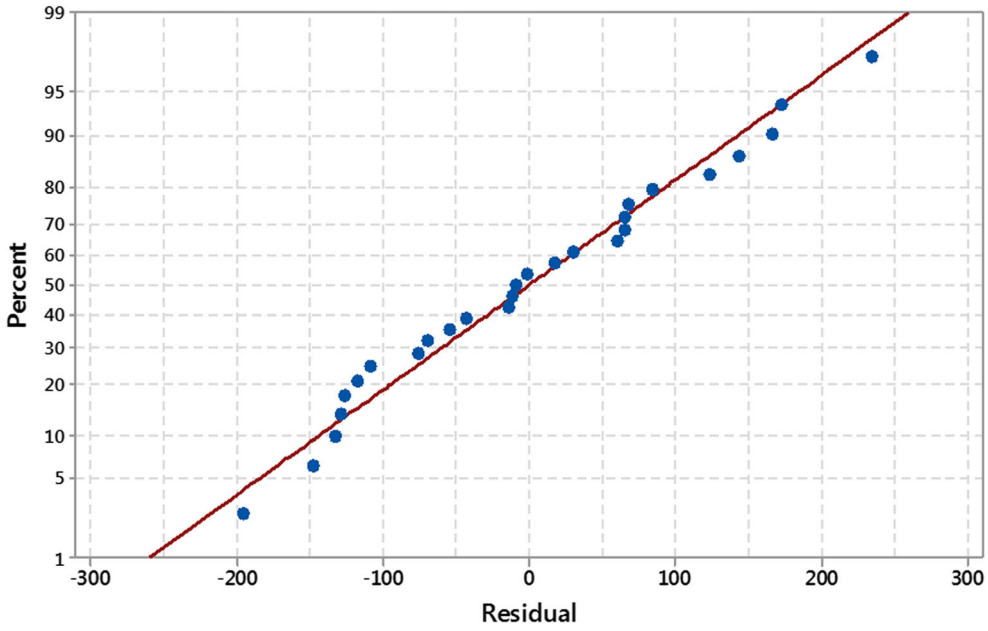

Fig. 7 Normal probability plot of the residuals for the response of deformation energy

also reduces the forming distance due to the increased step down, and leads to the decline of the deformation energy. The increased forming length is associated with the increased friction and heat dissipation. In terms of tool diameter, no obvious effect has been found on deformation energy since contributions from first-order, second-order and interaction effects may be counteracted among each other. Therefore, the optimum selection of tool size to minimise deformation energy depends on the values of other forming parameters.

3.3 Geometric accuracy

The formed components were scanned in the unclamped condition using a MINOLTA VIVID laser scanner, and their profiles were represented by a mass of point clouds. These profiles were then sectioned in the plane across the middle of the pyramid. For each test, the scanned profile was aligned with the designed shape at the outer undeformed region in the vertical direction. A comparison of the formed profile with the designed component shape is shown in Fig. 9.

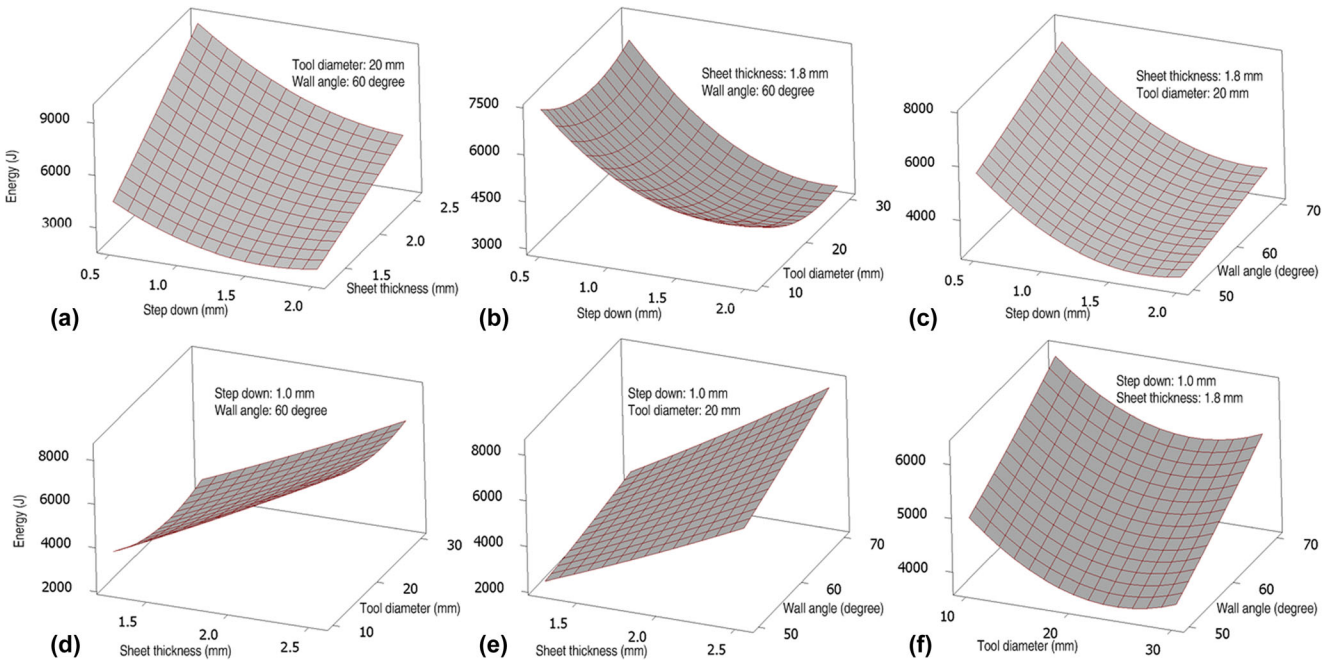

Fig. 8 Response surface plots of deformation energy by varying process parameters

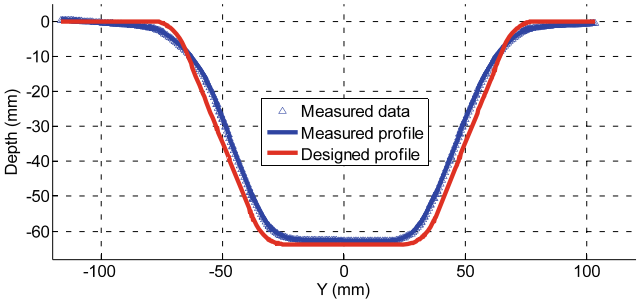

Fig. 9 Comparison between the measured and designed profiles

The global geometric error is defined by the average vertical deviation between the measured and designed profiles for all the points along the cross-section, and this global error is used for evaluating the geometric quality of the formed parts. In particular, the geometric error for the fractured parts (α=70°) is calculated as the vertical difference between the formed parts at the onset of material fracture to the intermediate shape corresponding the current tool path. It can be seen from Fig. 9 that although all the remaining regions were not formed to the targeted positions, the sheet was overformed at the transition area around the major diameter. The largest deviation was obtained at the side wall while good geometric accuracy was obtained for the bottom of the truncated pyramid.

A similar analysis procedure used for deformation energy was also performed. First, an empirical model described by a second-order response surface was obtained for the global geometric error,

$$\varepsilon_g = 3.671 + 0.285A + 0.627B + 0.302C - 0.447D - 0.403C^2 - 1.042D^2 + 0.473BC. \quad (4)$$

Table 4 presents the results of ANOVA for the response function surface and a probability P value less than 0.0001 indicates that the developed response function is adequate. Figure 10 shows a linear relation between the residuals and the percentage of the measurements that fall below these residuals, confirming that the experimental results are effective. Moreover, a value of 0.914 for predicted R^2 also suggests that the model can be reasonably used for future prediction.

According to the P value in Table 4 and the coefficients in Eq. (4), it can be seen that the quadratic effect of wall angle (D) is the most influential factor on the global error followed by the linear effect of sheet thickness (B), wall angle (D) and tool diameter (C) as well as step down (A). Furthermore, the interaction effect of sheet thickness and tool diameter (BC) also has considerable effect on global geometric error. To investigate the effect of each factor on the global geometric error in detail, response surfaces by varying the values of process parameters are plotted in Figs. 11 and 12. Overall, the

Table 4 Results of ANOVA for global geometric error (from Minitab)

Source	SS	DOF	MS	F value	P-value	Remarks
Model		14		9.11	<0.0001	Significant
A		1		6.99	0.021	Significant
B		1		33.77	<0.0001	Significant
C		1		7.84	0.016	Significant
D		1		17.13	0.001	Significant
A^2		1		0.37	0.556	
B^2		1		0.18	0.683	
C^2		1		6.19	0.029	Significant
D^2		1		41.40	<0.0001	Significant
AB		1		1.53	0.24	
AC		1		0.04	0.84	
AD		1		0.63	0.442	
BC		1		6.39	0.027	Significant
BD		1		1.33	0.272	
CD		1		0.50	0.495	
Residual		12				
Lack of fit		10		8.05		
Total		26				

geometric errors fall into the range from 1.5 to 4.5 mm for most of the cases.

As shown in Fig. 11, the response surfaces of global geometric error are constructed with sheet thickness and wall angle with different settings of step down and tool radius ranging from the lowest to highest levels. In all levels, the response of geometric error has the largest value when the pyramids with the wall angle of 60° are formed. By either reducing or increasing the wall angle, a better geometric accuracy can be achieved especially when the step down and tool radius are set as lower values as demonstrated in Fig. 11a. However, the following aspects need to be clarified in terms of the effect of wall angle. The difference of wall angles leads to the variation of the area ratio between the side wall and the bottom region of the formed parts. Considering that the average geometric error at the bottom region is smaller than that at the side wall, the calculation of the global error would be affected. Specifically, with larger wall angles, the side wall is steeper so the area ratio between bottom regions to side wall is increased under the same formed depth. Additionally, for the parts of 70° wall, sheets are not formed successfully to the designed depth of 65 mm but fracture earlier at a depth between 25 and 30 mm. This could also result in a higher area ratio between bottom region to side wall hence further reduce the geometric deviation due to the better geometric accuracy at the bottom region.

The sheet thickness also has a significant effect on the overall geometric accuracy. As shown in Fig. 11, greater global geometric accuracy can be attained with thinner sheets in

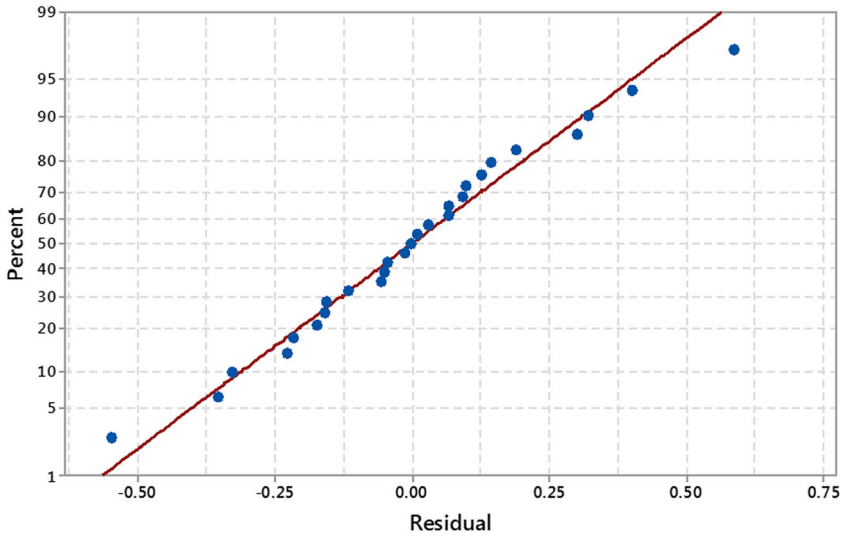

Fig. 10 Normal probability plot of the residuals for the response of global error

most of the conditions. This effect is evident especially when the step down and tool diameter were set as higher levels. This confirms the previous reported conclusion that the increase of the sheet thickness will result in higher geometric error at the bottom corner of the formed cone [16]. However, with small step-down value, small tool size but large wall angle (see Fig. 11a), increase of the thickness will contribute to a better geometric quality.

The selections of step down and tool diameter also have considerable effects on global geometric error according to *P* values in Table 4. Response surface plots with step down and tool diameter are presented in Fig. 12. For parts with thicker sheets and large wall angles, reducing the step-down size can be considered as an effective strategy to improve the geometric accuracy as also suggested in previous experimental work [19]. The reduced step-down size would result in a smaller transition zone between two adjacent contours which allows for a better control of the material deformation towards the targeted profile. However, the effect is not evident under smaller wall angle with thin sheets.

From Fig. 12, it can be seen that cases with medium step-down size and tool diameter tend to have poor geometric

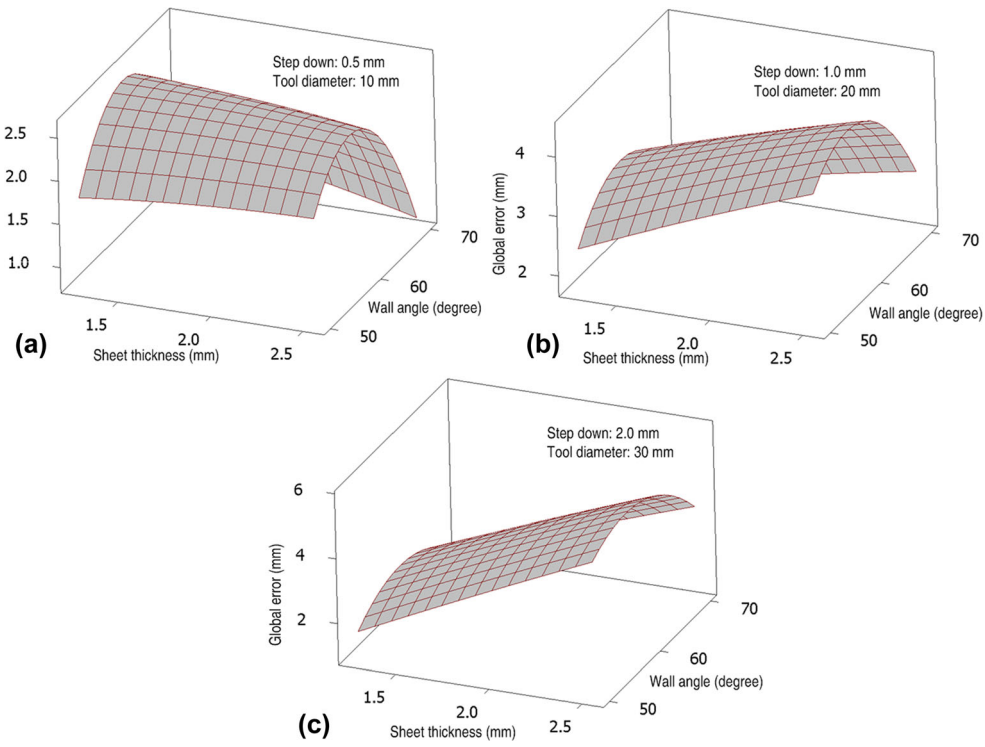

Fig. 11 Response surface plots of global geometric error in sheet thickness and wall angle

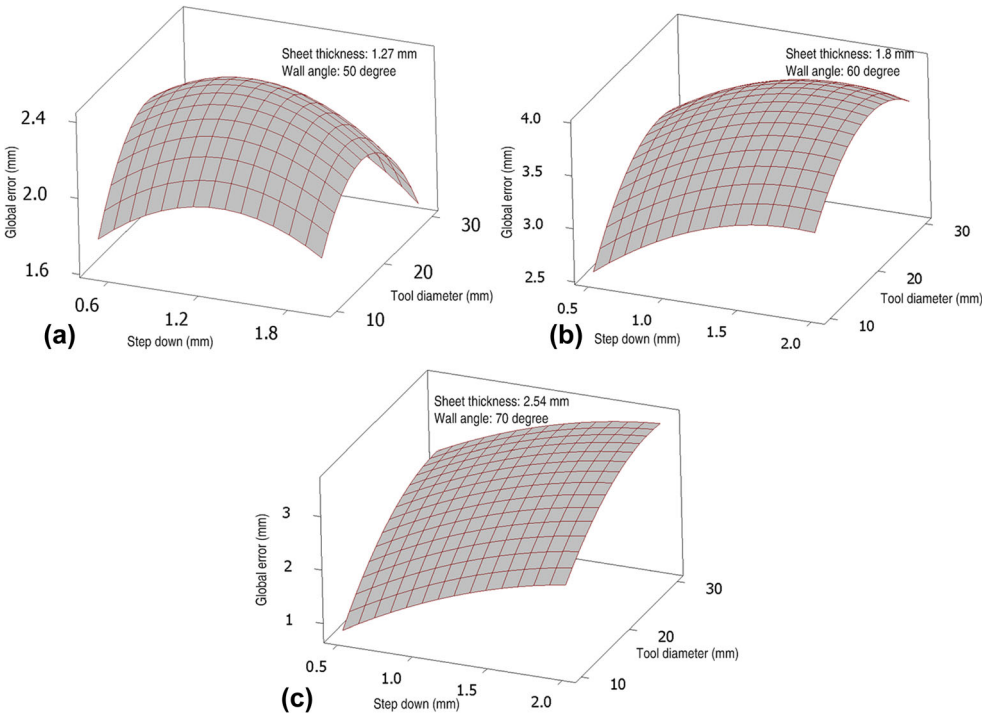

Fig. 12 Response surface plots of global geometric error in step down and tool diameter

accuracy. This was indicated in Eq. (4) by an extra quadratic term of tool diameter which leads to a non-linear effect on geometric error. Since the geometric error was measured under unclamped condition, the springback of the material plays a vital role in part inaccuracy after releasing forming load and boundary constraints. The membrane analysis by Silva etc. [28] suggested that the membrane stress is closely related with the ratio between thickness and tool radius. Due to the fact that the springback is caused by the release of residual stress, geometric accuracy is also affected by this ratio (as presented by the response surface from Fig. 12a to c). Furthermore, the interaction between thickness and tool diameter also has a non-ignorable effect as suggested by a low *P* value in Table 4. This is consistent with published work by Hussain et al. [29] that the ratio between tool diameter and sheet thickness has great influence on the ISF process in terms geometric accuracy and formability.

3.4 Optimisation

This section provides the optimisation results of both individual and simultaneous minimisation of deformation energy and geometric error during pyramid-forming processes. The desirability function in Minitab has been used to find the optimal setting. The desirability has a range of 0 to 1 and was used to evaluate how the settings optimise a response. First, an optimal setting condition for minimising the deformation energy was obtained. According to the range of the measured experimental results, the target value for the minimum deformation energy was set as 1000 J and the upper bound was set as 20, 000 J. Figure 13a presents the optimised condition for achieving minimum deformation energy. In this figure, the trend of the desirability with the changing of each parameter over its defined range is plotted in the first row. The second row illustrates the trend of the value of predicted deformation energy over the whole defined range for all four parameters. Since the purpose of this optimisation is to determine the lowest energy, a lower value of deformation energy corresponds to a higher value of desirability as presented in the figure. In particular, the values of the parameters for the optimal condition are indicated at the vertical lines and also presented within the square brackets. Accordingly, as shown in Fig. 13a, the optimal condition was determined as step down (1.59 mm), sheet thickness (1.27 mm), tool diameter (24.75 mm) and wall angle (50°), obtaining a minimum deformation energy of 1659 J. Similarly, with the setting of target value for geometric error at 0.1 mm and upper bound at 10 mm, the optimal condition was found to be (Fig. 13b) at a step down of 0.5 mm, sheet thickness of 2.54 mm, tool diameter of 10 mm and wall angle of 70°. Since all the parameters are set at their boundary values, it seems that only a local optimisation solution is obtained. The predicted minimum geometric error is 0.81 mm with a desirability of 0.931.

Finally, the optimal combination of process parameters for simultaneously minimisation of both deformation energy and geometric error has been studied by using the multi-response optimisation approach. In this approach, each of the response value is transformed using a specific desirability function. The

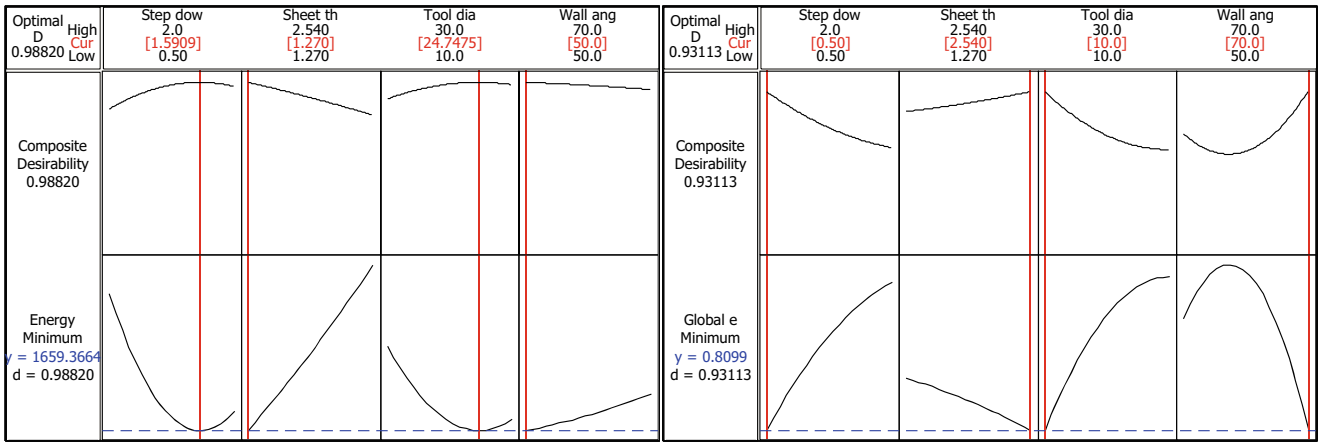

Fig. 13 Single response optimisation results for **a** deformation energy and **b** global geometric error (optimal parameters are indicated with *vertical lines*)

weight of each response can be determined by the user with the value from 0 to 1. This method includes three steps: (i) obtaining the individual desirability for each response, (ii) combining the individual desirability to obtain the combined or composite desirability and (iii) maximizing the composite desirability and identifying the optimal input variable settings [30]. The importance of these two responses is set as equal in the present study. As presented in Fig. 14, the trend of the composite desirability that combines geometric error and deformation energy is plotted in the first row. The trends of the predicted global geometric error and deformation energy over their whole defined range for all four parameters are illustrated in the second and third row, respectively. As indicated at the vertical lines, under the working condition with high step down of 2 mm, low sheet thickness of 1.27 mm, high tool diameter of 30 mm and large wall angle of 70°, a highest composite desirability of 0.917 can be achieved. The corresponding deformation energy and global geometric error are predicted to be 2459 J and 0.98 mm, respectively. The response surface method presented provides a useful guidance for optimal process design in terms of deformation energy and geometric error.

Under the actual forming condition, sheet thickness may need to be defined by other design parameters rather than optimisation. Therefore, the optimisation of both deformation energy and geometric error for a range of sheet thicknesses has been performed and tabulated in Table 5. It can be seen that, in the tested range, the selection of sheet thickness has no effect on the optimum setting of step down, tool diameter and wall angle, but greatly influences the required deformation energy and part geometric accuracy. Both the energy and geometric error increase largely with the increase of original sheet

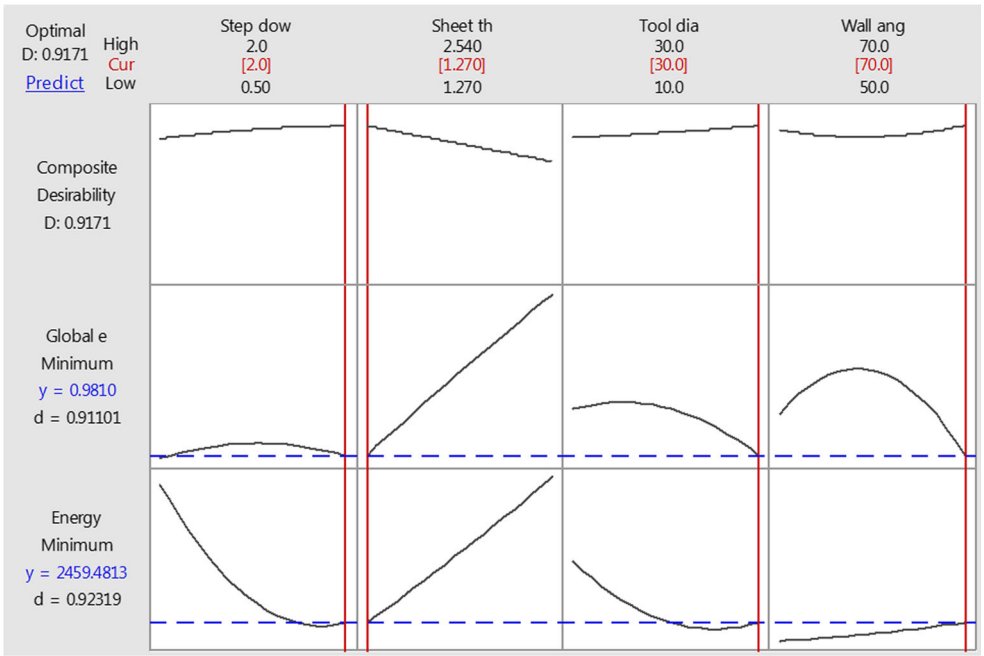

Fig. 14 Multi-responses optimisation result for both deformation energy and global geometric error (optimal parameters are indicated with *vertical lines*)

Table 5 Optimised results for deformation and geometric error under different sheet thickness

Sheet thickness (mm)	Optimised results					
	Step down (mm)	Tool diameter (mm)	Wall angle (°)	Composite desirability	Minimum energy (J)	Minimum error (mm)
1.27	2.0	30	70	0.917	2459	0.98
1.8	2.0	30	70	0.828	3693	2.09
2.54	2.0	30	70	0.702	5610	3.56

thickness. Consequently, reducing the sheet thickness will not only save the cost of material and energy consumption but also improve the part geometric quality in the ISF process.

4 Conclusions and future work

In this study, the effects of the four key process parameters on deformation energy and geometric accuracy in ISF have been investigated by performing a Box-Behnken design. Quadratic statistical models have been developed to predict the values of deformation energy and geometric error under different settings of the process parameters. Moreover, the optimum working conditions are determined to achieve minimum energy and geometric error using response surface methodology with desirability functions. The main conclusions from this study are drawn as follows:

- Response surface methodology with Box-Behnken design was successfully applied to investigate the effects of step down, sheet thickness, wall angle and tool diameter on both deformation energy and geometric accuracy during pyramid-forming processes. Statistical models have been established considering both quadratic and linear effects of most influential forming parameters.
- The deformation energy during the forming process was calculated based on measured forming forces. It was found that the deformation energy heavily depends on the sheet thickness because of higher plastic energy required to deform the material. Increasing step-down size with a limited range or decreasing the wall angle is an effective approach to reduce the deformation energy.
- The global geometry error defined by the vertical distance between the formed and designed profiles is selected as the measure of the geometric accuracy. It was concluded that the accuracy is largely determined by the quadratic effect of wall angle, the linear effect of sheet thickness and the interaction effect of thickness and step down. Decreasing the step-down size was found always helpful to improve the geometric accuracy.
- The optimisation results for both independent and simultaneous minimisation of deformation energy and geometric error during the pyramid-forming process are provided. Under the working condition with high step down of 2 mm, low sheet thickness of 1.27 mm, high tool diameter of 30 mm and large wall angle of 70°, the deformation energy and global geometric error are expected to be minimised to 2459 J and 0.98 mm, respectively.

Some suggestions for future investigation are provided,

- The deformation energy was calculated from forming forces during the forming operations. Actually, the total process energy may include the components related to idle times and relevant auxiliary operations and also machine tool inefficiencies during production mode: electrical losses, mechanical losses, etc. A comprehensive evaluation for the total consumed energy could be employed in further study.
- In this study, the global geometric error was used as the indicator for evaluating the geometric quality while in some cases the tolerances at some particular positions may be of interest instead.
- It is known that increasing the feed rate (forming speed) will save the required energy due to the reduced forming time, but this may affect the part accuracy as reported in [25]. An optimum value for the feed rate needs to be found so that the energy can be greatly saved without sacrificing part quality.

Acknowledgments The present work was supported by the Australian Research Council (ARC) Linkage project, Boeing Research and Technology Australia (BRTA) and QMI Solutions. China Scholarship Council (CSC) is also acknowledged for the scholarship support.

Funding This study was funded by Australian Research Council (ARC) Linkage project (grant number LP100200689).

Conflict of interest Yanle Li has received scholarship from China Scholarship Council (CSC). Haibo Lu has received scholarship from China Scholarship Council (CSC).

Ethical statement The authors declare that the manuscript follows the ethical statement of the International Journal of Advanced Manufacturing Technology. The manuscript has not been submitted to more than one journal for simultaneous consideration and has not been published partly or full previously.

References

1. Jeswiet J, Micari F, Hirt G, Bramley A, Duflou J, Allwood J (2005) Asymmetric single point incremental forming of sheet metal. Annal Manuf Technol 54(2):623–649
2. Echrif SBM, Hrairi M (2011) Research and progress in incremental sheet forming processes. Mater Manuf Process 26(11):1404–1414. doi:10.1080/10426914.2010.544817
3. Duflou JR, Sutherland JW, Dornfeld D, Herrmann C, Jeswiet J, Kara S, Hauschild M, Kellens K (2012) Towards energy and resource efficient manufacturing: a processes and systems approach. CIRP Ann Manuf Technol 61(2):587–609. doi:10.1016/j.cirp.2012.05.002
4. Dittrich MA, Gutowski TG, Cao J, Roth JT, Xia ZC, Kiridena V, Ren F, Henning H (2012) Exergy analysis of incremental sheet forming. Prod Eng 6(2):169–177. doi:10.1007/s11740-012-0375-9
5. Branker K, Adams D, Jeswiet J (2012) Initial analysis of cost, energy and carbon dioxide emissions in single point incremental forming - producing an aluminium hat. Int J Sustain Eng 5(3):188. doi:10.1080/19397038.2011.634033
6. Ingarao G, Ambrogio G, Gagliardi F, Di Lorenzo R (2012) A sustainability point of view on sheet metal forming operations: material wasting and energy consumption in incremental forming and stamping processes. J Clean Prod 29–30:255–268. doi:10.1016/j.jclepro.2012.01.012
7. Ingarao G, Vanhove H, Kellens K, Duflou JR (2014) A comprehensive analysis of electric energy consumption of single point incremental forming processes. J Clean Prod 67:173–186. doi:10.1016/j.jclepro.2013.12.022
8. Aerens R, Eyckens PV, Bael A, Duflou JR (2010) Force prediction for single point incremental forming deduced from experimental and FEM observations. Int J Adv Manuf Technol 46(9):969–982
9. Ambrogio G, Ingarao G, Gagliardia F, Di Lorenzo R (2014) Analysis of energy efficiency of different setups able to perform single point incremental forming (SPIF) processes. Procedia CIRP 15:111–116. doi:10.1016/j.procir.2014.06.055
10. Bagudanch I, Garcia-Romeu ML, Ferrer I, Lupiañez J (2013) The effect of process parameters on the energy consumption in single point incremental forming. Procedia Eng 63:346–353. doi:10.1016/j.proeng.2013.08.208
11. King JM, Allwood GPF, Duflou J (2005) A structured search for applications of the incremental sheet-forming process by product segmentation. Proc Inst Mech Eng B J Eng Manuf 219(2):239–244. doi:10.1243/095440505x8145
12. Braun JM, Allwood D, Music O (2010) The effect of partially cut-out blanks on geometric accuracy in incremental sheet forming. J Mater Process Technol 210(11):1501–1510. doi:10.1016/j.jmatprotec.2010.04.008
13. Micari F, Ambrogio G, Filice L (2007) Shape and dimensional accuracy in Single Point Incremental Forming: state of the art and future trends. J Mater Process Technol 191(1–3):390–395. doi:10.1016/j.jmatprotec.2007.03.066
14. Essa K, Hartley P (2011) An assessment of various process strategies for improving precision in single point incremental forming. Int J Mater Form 4(4):401–412. doi:10.1007/s12289-010-1004-9
15. Guzmán CF, Gu J, Duflou J, Vanhove H, Flores P, Habraken AM (2012) Study of the geometrical inaccuracy on a SPIF two-slope pyramid by finite element simulations. Int J Solids Struct 49(25):3594–3604. doi:10.1016/j.ijsolstr.2012.07.016
16. Ambrogio G, Cozza V, Filice L, Micari F (2007) An analytical model for improving precision in single point incremental forming. J Mater Process Technol 191(1–3):92–95. doi:10.1016/j.jmatprotec.2007.03.079
17. Ham MEJ (2007) Single point incremental forming of aluminum sheet metal: the development of maximum forming angle forming limits, measured strains, surface roughness and dimensional accuracy. Ph.D., Queen's University (Canada), Ann Arbor
18. Skjoedt MB, Silva M, Martins PAF, Bay N (2008) Revisiting the fundamentals of single point incremental forming by means of membrane analysis. Int J Mach Tools Manuf 48(1):73–83. doi:10.1016/j.ijmachtools.2007.07.004
19. Lu H, Li Y, Liu Z, Liu S, Meehan PA (2014) Study on step depth for part accuracy improvement in incremental sheet forming process. Adv Mater Res 939:274–280. doi:10.4028/www.scientific.net/AMR.939.274
20. Mourabet M, El Rhilassi A, El Boujaady H, Bennani-Ziatni M, Taitai A (2013) Use of response surface methodology for optimization of fluoride adsorption in an aqueous solution by Brushite. Arab J Chem. doi:10.1016/j.arabjc.2013.12.028
21. Mourabet M, El Rhilassi A, El Boujaady H, Bennani-Ziatni M, El Hamri R, Taitai A (2012) Removal of fluoride from aqueous solution by adsorption on Apatitic tricalcium phosphate using Box–Behnken design and desirability function. Appl Surf Sci 258(10):4402–4410. doi:10.1016/j.apsusc.2011.12.125
22. Liu Z, Liu S, Li Y, Meehan PA (2014) Modeling and optimization of surface roughness in incremental sheet forming using a multi-objective function. Mater Manuf Process 29(7):808–818. doi:10.1080/10426914.2013.864405
23. Bhattacharya A, Maneesh K, Venkata Reddy N, Cao J (2011) Formability and surface finish studies in single point incremental forming. J Manuf Sci Eng 133(6):61020. doi:10.1115/1.4005458
24. Natarajan U, Periyanan P, Yang S (2011) Multiple-response optimization for micro-endmilling process using response surface methodology. Int J Adv Manuf Technol 56(1–4):177–185
25. Ambrogio G, Filice L, Gagliardi F (2012) Improving industrial suitability of incremental sheet forming process. Int J Adv Manuf Technol 58(9–12):941–947. doi:10.1007/s00170-011-3448-6
26. Li Y, Daniel WJT, Liu Z, Lu H, Meehan PA (2015) Deformation mechanics and efficient force prediction in single point incremental forming. J Mater Process Technol. doi:10.1016/j.jmatprotec.2015.02.009
27. Li Y, Liu Z, Lu H, Daniel WJT, Liu S, Meehan P (2014) Efficient force prediction for incremental sheet forming and experimental validation. Int J Adv Manuf Technol 73(1–4):571–587. doi:10.1007/s00170-014-5665-2
28. Silva MB, Nielsen PS, Bay N, Martins PAF (2011) Failure mechanisms in single-point incremental forming of metals. Int J Adv Manuf Technol 56(9):893–903. doi:10.1007/s00170-011-3254-1
29. Hussain G, Khan HR, Gao L, Hayat N (2012) Guidelines for tool-size selection for single-point incremental forming of an aerospace alloy. Mater Manuf Process 28(3):324–329. doi:10.1080/10426914.2012.700151
30. What is response optimization. (2014). http://support.minitab.com/